IEEE Access
Multidisciplinary | Rapid Review | Open Access Journal

Received April 8, 2019, accepted April 28, 2019, date of publication May 1, 2019, date of current version May 15, 2019.

*Digital Object Identifier 10.1109/ACCESS.2019.2914268*

# A Novel Blind Spectrum Sensing Technique for Multi-User Ultraviolet Communications in Atmospheric Turbulence Channel

**SUDHANSHU ARYA, (Student Member, IEEE), AND YEON HO CHUNG, (Senior Member, IEEE)**
Department of Information and Communications Engineering, Pukyong National University, Busan 48513, South Korea

Corresponding author: Yeon Ho Chung (yhchung@pknu.ac.kr)

This work was supported by the Basic Science Research Program through the National Research Foundation of Korea (NRF) funded by the Ministry of Education under 2018R1D1A3B07049858.

**ABSTRACT** One of the primary challenges in multi-user free space optical wireless systems is to periodically sense the optical frequency spectrum at the receiver to identify whether the channel is occupied by other transceiver pairs in order to avoid interference. Spectrum sensing enables the user to continuously monitor the channel prior to its access to the channel. In this paper, we propose a novel blind spectrum sensing scheme for an unknown ultraviolet signal over strong atmospheric turbulence channel, based on the estimated signal-to-noise ratio (SNR) and the noise power. We derive this estimated SNR and the noise power from a statistical ratio of the received signal. The turbulence effect causes fluctuations in the received signal intensity, resulting in power loss at the receiver. Taking this negative effect into account, the blind SNR-based spectrum sensing scheme is equipped with spatial diversity scheme in the form of switch-and-stay combining. The intensity fluctuations are modeled by a gamma-gamma distribution. Based on the estimated SNR and noise power expressions, novel closed-form expressions for the probability of detection and the probability of false alarm are derived. It is also found that sensing capability is enhanced with the diversity scheme.

**INDEX TERMS** Gamma-gamma turbulence, spectrum sensing, ultraviolet.

## I. INTRODUCTION

The need for high data rate, improved security, and low power transmission has geared attention toward the optical spectrum including infrared and ultraviolet (UV) band which offer huge unregulated bandwidth, security, and cost-effective communication, compared with radio frequency based communication systems [1], [2]. Atmospheric scattering at the UV wavelengths is larger than in other optical wavelengths, and, as a result, in non-line-of-sight (NLOS) communications links, the receiver can receive more power from the transmitter than other portions of the optical band [3], [4], thereby making it an interesting choice for NLOS links.

As optical wireless systems communicate in the unlicensed band, the receiver must find available frequency band before transmission in order to avoid the interference from other potential transceiver pairs available in that region. A generalized likelihood ratio test (GLRT) based spectrum sensing approach was proposed for optical wireless scattering communication [5]. The authors proposed two detection rules, namely, the sum-counting test and the general GLRT. The scheme is found to be optimal for spectrum sensing with unknown parameters based on finite samples. Though the general GLRT outperforms the sum-counting test, it is found to have higher computational complexity. A less complex sequential detection based spectrum sensing for optical wireless scattering communications was reported [6]. This scheme adapts the sample size to the present channel realization. To reduce the computational complexity, a one-term approximation of the log-likelihood ratio (LLR) computation was presented. This approximation leads to fewer samples required than the exact LLR computation.

One of the channel impairments that an optical signal experiences is turbulence. The turbulence may degrade the communication link performance as the link range extends. As the result of random variations of the refractive index, the intensity of the UV signal fluctuates at the receiver. In this

The associate editor coordinating the review of this manuscript and approving it for publication was Emrecan Demirors.

paper, to model the received signal fluctuations, we consider the Gamma-Gamma distribution due to its excellent agreement between experimental and theoretical results in a wide range of turbulence conditions [7]–[9]. This model is a two-parameter distribution which is based on a doubly stochastic theory of scintillation, and assumes that small-scale irradiance fluctuations are modulated by large-scale irradiance fluctuations of the propagating wave, both governed by independent gamma distributions. For UV communication links, the Gamma-Gamma distribution can be directly related to the atmospheric parameters defining turbulence conditions [10], [11].

In this paper, we present a novel blind spectrum sensing technique for multi-user UV communication systems operating in the turbulence atmospheric channel. We derive the SNR and noise power estimates based on a statistical ratio of the receive data when the channel undergoes gamma-gamma fading. The proposed scheme does not require any information about the channel or the UV signal to be detected and is robust to unknown dispersive optical channel. Thus, it is a blind spectrum sensing technique over the turbulence atmospheric UV channel. We consider the on-off keying (OOK) transmission format and present an analytical approach for the probability of detection and the probability of false alarm over Gamma-Gamma distributed atmospheric turbulence channel. We also quantify the improvement in the proposed system with a low complex switch-and-stay combining (SSC) diversity scheme. Although this approach can also be used in line-of-sight (LOS) link, in this paper we focus on NLOS UV communication systems relying on atmospheric scattering.

The rest of this paper is organized as follows. In Section II, we provide the system model and the receiver structure. A blind SNR estimation procedure in gamma-gamma fading channel is presented in Section III. In Section IV, based on the estimated SNR and noise power, the closed-form expressions for the probability of detection and the probability of false alarm are evaluated under gamma-gamma turbulence fading. Simulation results are given in Section V, and finally, conclusions are drawn in Section VI.

## II. SYSTEM MODEL

Consider an NLOS UV link geometry as depicted in Fig. (1). The transmitter and the receiver are separated by a baseline distance $d$. We employ a SSC combiner with dual branches. These two branches provide the diversity gain to the proposed system. The proposed system model with SSC diversity scheme is shown in Fig. (2).

The statistical channel model is given by

$$\begin{aligned} y_i &= SP_r I_i + w_i, \quad H_1 \\ &= w_i, \quad H_0, \end{aligned} \tag{1}$$

where $y_i$ is the instantaneous photocurrent at the $i^{th}$ receiver with $i = 1, 2$. $S$ represents each receiver responsivity, $I_i$ denotes the intensity fluctuations in the $i^{th}$ branch due to the atmospheric turbulence and $w_i$ is the additive white Gaussian noise (AWGN) with zero mean and variance $\sigma_n^2$. $H_0$ and $H_1$ represent the two hypotheses of the UV signal absence and presence, respectively. $P_r$ is the received optical power equal to $P_t \times P_L$, where $P_t$ is the transmitting power and $P_L$ is the UV channel path loss given by [12]

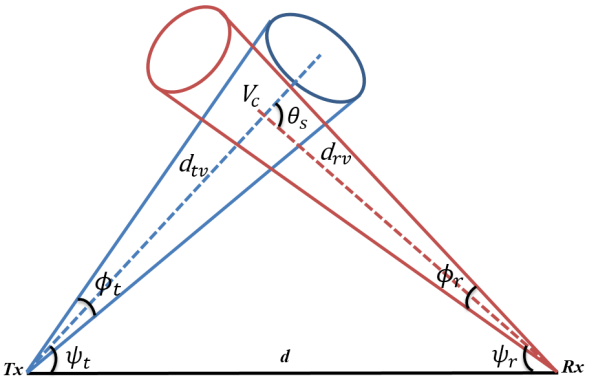


**FIGURE 1.** NLOS UV scattered communication system.

$$P_L = \frac{\alpha_s q_s A_r \phi_t^2 \phi_r \sin(\theta_s) \left(12 \sin^2 \psi_r + \phi_r^2 \sin^2 \psi_t\right)}{192 d \sin \psi_t \sin^2 \psi_r \sin^2 \frac{\phi_t}{4} \exp\left(\frac{\alpha_t d (\sin \psi_t + \sin \psi_r)}{\sin \psi_r}\right)}, \tag{2}$$

where $A_r$ is the effective area of the receiving aperture and $q_s$ represents the scattering phase function. $\theta_s$ is the scattering angle. $\phi_t$ is the transmitter beam angle and $\phi_r$ represents the receiver field-of-view (FOV), whereas $\psi_t$ and $\psi_r$ denote the transmitter and the receiver apex angles, respectively. $\alpha_t$ is the total extinction coefficient and is the sum of the scattering coefficient $\alpha_s$ and the absorption coefficient $\alpha_a$. $V_c$ in Fig. (1) represents the common volume between the transmitter beam and the receiver FOV.

The intensity fluctuations are modeled by the gamma-gamma distribution that is theoretically valid under all fluctuation conditions [7]. The probability density function (PDF) of the irradiance fluctuations following gamma-gamma distribution is given by

$$f_I(I) = \frac{2 (ab)^{\left(\frac{a+b}{2}\right)}}{\Gamma(a) \Gamma(b)} I^{\left(\frac{a+b-2}{2}\right)} K_{a-b}\left(2\sqrt{abI}\right), \tag{3}$$

where $\Gamma(\cdot)$ represents the Gamma function and $K_{a-b}(\cdot)$ is the modified Bessel function of the second kind of order $(a-b)$. For plane wave optical radiation, the parameters $a$ and $b$ are given by [8]

$$a = \left[\exp\left(\frac{0.49\delta^2}{\left(1 + 1.11\delta^{12/5}\right)^{7/6}}\right) - 1\right]^{-1} \tag{4}$$

and

$$b = \left[\exp\left(\frac{0.51\delta^2}{\left(1 + 0.69\delta^{12/5}\right)^{5/6}}\right) - 1\right]^{-1}, \tag{5}$$

where $\delta = 1.23 C_n^2 k^{7/6} d_{LOS}^{11/6}$ is the log irradiance variance. Here, $k = 2\pi/\lambda$ is the wave number, $\lambda$ is the UV wavelength,

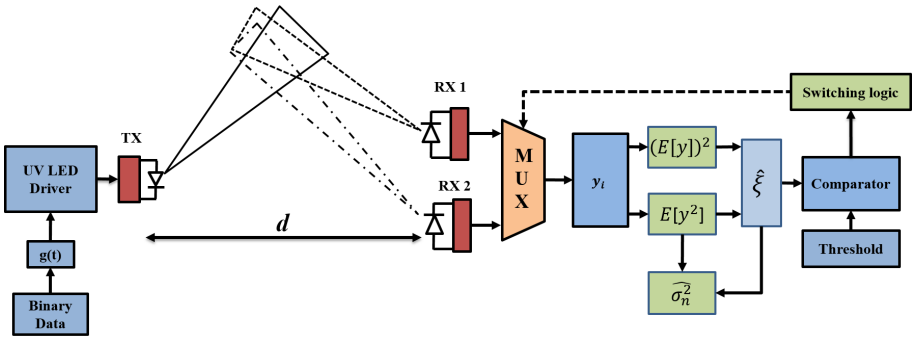


**FIGURE 2.** Proposed system model: SNR based spectrum sensing for UV scattered communication system.

$C_n^2$ stands for the refractive index structure coefficient and is a measure of the strength of the optical turbulence. In general, the values of $C_n^2$ vary between $10^{-15}$ and $10^{-12}$ $m^{-2/3}$. The latter value represents the strong turbulence [25]. $d_{LOS}$ represents the LOS propagation distance.

The NLOS UV link geometry consists of two LOS paths: one from the transmitter to common volume, and the other from the common volume to the receiver. For each path, we can use the Gamma-Gamma distribution to model the irradiance fluctuations and then combine the two LOS results to obtain a NLOS turbulence distribution [13], [14]. The irradiance fluctuations in the UV signal arriving in the common volume follow the Gamma-Gamma distribution with the probability density function (PDF) given by

$$f_{I_V}(I_V) = \frac{2\left(a_V b_V\right)^{\left(\frac{a_V+b_V}{2}\right)}}{\Gamma(a_V)\,\Gamma(b_V)} I^{\left(\frac{a_V+b_V-2}{2}\right)} K_{a_V-b_V}\left(2\sqrt{a_V b_V I}\right), \tag{6}$$

where the parameters $a_V$ and $b_V$ can be calculated using (4) and (5) with $d_{LOS}$ substituted by $d_{tv}$. With the scattered photons acting as a new source towards the receiver, the conditional distribution of the irradiance fluctuations at the receiver is then given by

$$f_{I_R}(I_R|I_V) = \frac{2\left(a_R b_R\right)^{\left(\frac{a_R+b}{2}\right)}}{\Gamma(a_R)\,\Gamma(b_R)} I_R^{\left(\frac{a_R+b_R-2}{2}\right)} K_{a_R-b_R}\left(2\sqrt{a_R b_R I_R}\right), \tag{7}$$

where the parameters $a_R$ and $b_R$ can then be calculated using (4) and (5) with $d_{LOS}$ substituted by $d_{rv}$. The joint PDF of $I_V$ and $I_R$ is given by $f_{I_V,I_R}(I_V, I_R) = f_{I_R}(I_R|I_V) f_{I_V}(I_V)$. The marginal PDF of the irradiance fluctuations at the receiver is given by

$$f_{I_R}(I_R) = \int_0^\infty f_{I_R}(I_R|I_V) f_{I_V}(I_V)\, dI_V, \quad I_V > 0. \tag{8}$$

Substituting (6) and (7) into (8) and following the derivation steps provided in Appendix A, we can obtain the PDF of $I_R$ as

$$f_{I_R}(I_R) = \frac{\left(a_V b_V\right)\left(a_R b_R\right)^{\left(\frac{a_R+b_R}{2}\right)}}{\Gamma(a_V)\,\Gamma(b_V)\,\Gamma(a_R)\,\Gamma(b_R)} \times I_R^{\left(\frac{a_R+b_R-2}{2}\right)} G_{0,2}^{2,0}\left[a_R b_R I_R \,\middle|\, \frac{a_R-b_R}{2}, -\frac{a_R-b_R}{2}\right], \tag{9}$$

where $G_{u,v}^{s,t}[\cdot]$ represents the Meijer's G-function.

## III. BLIND SNR AND NOISE POWER ESTIMATION

The proposed system model with SSC diversity scheme is depicted in Fig. (2). We first develop an approach to estimate the average received SNR. This will then lead to derive the performance metrics associated with the spectrum sensing for a UV communication system.

### A. SNR ESTIMATION

The instantaneous electrical SNR $\chi_i$ at the $i^{th}$ branch given by

$$\chi_i = \frac{S^2 P_r^2 I_{Ri}^2}{2\sigma_n^2}, \quad i = 1, 2. \tag{10}$$

We aim to estimate the average received SNR defined as

$$\xi = \frac{S^2 P_r^2 E\left[I_{Ri}^2\right]}{2\sigma_n^2}. \tag{11}$$

As in [15], we specify a parameter $\beta$ as the ratio of two statistical computations on the measurement of the received signal as

$$\beta = \frac{E\left[y^2\right]}{(E[y])^2}. \tag{12}$$

$E\left[y^2\right]$ is derived as

$$E\left[y^2\right] = E\left[(SP_r I_{Ri} + w)^2\right] = S^2 P_r^2 E\left[I_{Ri}^2\right] + E\left[w^2\right] + 2SP_r E\left[I_{Ri}\right] E[w]. \tag{13}$$

After following the steps provided in Appendix B, the closed-form expression of $E\left[y^2\right]$ is obtained as

$$E\left[y^2\right] = \frac{S^2 P_r^2 \left(a_V b_V\right)}{2\Gamma\left(a_V\right)\Gamma\left(b_V\right)} \left(\frac{a_R+2}{a_R^2}\right)\left(\frac{b_R+2}{b_R^2}\right) + \sigma_n^2. \tag{14}$$

To find the expected value of $y$, we first average $y$ over a random variable $P_r$, then average over $w$ conditioned on $I$, and finally average over $I$. Following the steps provided in Appendix C, the closed-form expression of $E[y]$ is obtained as

$$E\left[y_i\right] = \frac{S P_r \left(a_V b_V\right)}{2\Gamma\left(a_V\right)\Gamma\left(b_V\right)\Gamma\left(a_R\right)\Gamma\left(b_R\right)} \left\{\frac{1}{a_R} + \frac{1}{b_R} + 1\right\}. \tag{15}$$

Substituting (14) and (15) into (12), the parameter $\beta$ is readily obtained as

$$\beta = \left(\frac{\xi+1}{\xi}\right) \times \frac{2\left(a_R+2\right)\left(b_R+2\right)\Gamma\left(a_V\right)\Gamma\left(b_V\right)\left[\Gamma\left(a_R\right)\Gamma\left(b_R\right)\right]^2}{\left(a_V b_V\right)\left(a_V+b_V+a_R+b_R\right)^2}. \tag{16}$$

For a given value of $\beta$ computed from the observation of $y_i$, the corresponding estimate of the average received SNR $\xi$ can readily be obtained from (16) as

$$\xi = \left\{\frac{\beta(a_V b_V)(a_V+b_V+a_R+b_R)^2}{2(a_R+2)(b_R+2)\Gamma(a_V)\Gamma(b_V)[\Gamma(a_R)\Gamma(b_R)]^2} - 1\right\}^{-1}. \tag{17}$$

### B. NOISE POWER ESTIMATION

In this section, we propose the estimation of noise power from the estimated parameter $\beta$. Using (11), (14), and (36), we obtained

$$E\left[y^2\right] = \left(\hat{\xi}+1\right)\hat{\sigma_n^2}. \tag{18}$$

Substituting (17) into (18) and after some mathematical manipulation the noise variance can then be estimated as

$$\hat{\sigma_n^2} = \frac{E\left[y^2\right]}{\left\{\frac{\beta(a_V b_V)(a_V+b_V+a_R+b_R)^2}{2(a_R+2)(b_R+2)\Gamma(a_V)\Gamma(b_V)[\Gamma(a_R)\Gamma(b_R)]^2} - 1\right\}^{-1} + 1}. \tag{19}$$

## IV. PERFORMANCE ANALYSIS

### A. PROBABILITY OF FALSE ALARM

The probability of false alarm $P_f$ is defined as the probability of the receiver, declaring that the optical spectrum is occupied by another transceiver pair even though the spectrum is actually unoccupied. The lower this probability is, the more likely the optical channel can be reused when it is free. We define the probability of false alarm as

$$P_f = P_r\left(T > \sigma_{n,Th}^2 \,|H_0\right) = 1 - F_T\left(\sigma_{n,Th}^2 \,|H_0\right), \tag{20}$$

where $T \triangleq y^2$ is the test statistics for the probability of false alarm and $\sigma_{n,Th}^2$ is the noise threshold level. $F_T$ represents the commutative distribution function (CDF) of the received signal under hypothesis $H_0$. Under hypothesis $H_0$ when only noise is present, $T$ follows a chi-squared distribution with one degree of freedom. The PDF of this random variable is given by

$$f_T\left(T\right) = \frac{1}{\Gamma\left(\frac{1}{2}\right)\sqrt{2\hat{\sigma_n^2}\,T}} \exp\left(-\frac{T}{2\hat{\sigma_n^2}}\right). \tag{21}$$

Making use of [16, eqs. 3.361.1 and 3.321.1] and [17, eq. 2.3-23], the probability of false alarm is derived as

$$p_f = 1 - \sum_{k=0}^{\infty} \frac{(-1)^k}{(2k+1)k!}\left(\frac{\sigma_{n,Th}^2}{2\hat{\sigma_n^2}}\right). \tag{22}$$

Note that $P_f$ is not related to the SNR because there is no signal.

### B. PROBABILITY OF DETECTION

The probability of detection $P_d$ is described as the probability of a receiver, declaring that the spectrum is occupied by another transceiver pair when the spectrum is indeed occupied by another transceiver pair. Mathematically, $P_d$ can be represented as

$$P_d = P_r\left(\chi > \chi_{Th} \,|H_1\right) = 1 - F_{SSC}\left(\chi \,|H_1\right), \tag{23}$$

where $\chi_{Th}$ is the detection threshold.

$F_{SSC}\left(\chi \,|H_1\right)$ is the CDF of $\chi$ conditioned on $H_1$. To analyze the performance of the SSC receiver, the CDF of the final (SSC combiner output) is required. Assuming that the selection of the two branches of the SSC receiver is mutually exclusive, the CDF of the final output is defined as [24]

$$F_{SSC}\left(\chi\right) = \begin{cases} F_{\chi_1,\chi_2}\left(\chi, \chi_{S_{Th}}\right), & \chi \le \chi_{S_{Th}} \\ F_{\chi_i}\left(\chi\right) - F_{\chi_i}\left(\chi_{S_{Th}}\right) + F_{\chi_1,\chi_2}\left(\chi, \chi_{S_{Th}}\right), & \chi > \chi_{S_{Th}}, \end{cases} \tag{24}$$

where $\chi_{S_{Th}}$ is the switching threshold and $F_{\chi_i}\left(\chi\right)$ is the CDF of $\chi_i$ and is readily derived as

$$F_{\chi_i}\left(\chi\right) = \left(\frac{a_V b_V}{\Gamma\left(a_V\right)\Gamma\left(b_V\right)}\right)^{\left(\frac{a_R+b_R+4}{4}\right)} \frac{\left[\left(a_R+2\right)\left(b_R+2\right)\right]^{\left(\frac{a_R+b_R}{4}\right)}}{\Gamma\left(a_V\right)\Gamma\left(b_V\right)} \times G_{1,3}^{2,1}\left[\sqrt{\frac{a_V b_V\left(a_R+2\right)\left(b_R+2\right)\chi}{\Gamma\left(a_V\right)\Gamma\left(b_V\right)\xi}} \times \left| \begin{matrix} 1-\frac{a_R+b_R}{4} \\ \frac{a_R-b_R}{2}, \frac{b_R-a_R}{2}, -\frac{a_R+b_R}{4} \end{matrix} \right.\right] \times \left(\frac{\chi}{\xi}\right)^{\left(\frac{a_R+b_R}{4}\right)}. \tag{25}$$

For the derivation of (25), see Appendix D.

$F_{\chi_1,\chi_2}\left(\chi, \chi_{S_{Th}}\right)$ in (24) is defined as

$$F_{\chi_1,\chi_2}\left(\chi, \chi_{S_{Th}}\right) = \int_0^{\chi}\int_0^{\chi_{S_{Th}}} f_{\chi_1,\chi_2}\left(\chi_1, \chi_2\right) d\chi_1 d\chi_2, \quad (26)$$

where $f_{\chi_1,\chi_2}\left(\chi_1, \chi_2\right)$ is the joint PDF of the instantaneous SNR at each branch of the SSC receiver.

As a result of the close proximity of the photodiodes, there occurs a correlation between the received signals. Both, the large- and small-scale fading contribute to the correlation. For $L$ apertures, the autocorrelation matrix of order $(L \times L)$ is defined as [19]

$$\mathbf{R}_\rho = \frac{a\mathbf{R}_Y + b\mathbf{R}_X + \mathbf{R}_X \odot \mathbf{R}_Y}{a+b+1}, \quad (27)$$

where $\mathbf{R}_X$ and $\mathbf{R}_Y$ are the autocorrelation matrices corresponding to large- and small-scale fading, respectively. Provided the independent fading, the correlation coefficient between two apertures can then be written as [20]

$$\rho = \frac{a\rho_Y + b\rho_X + \rho_X\rho_Y}{a+b+1}, \quad (28)$$

where $\rho_X$ and $\rho_Y$ are the correlations among large- and small-scale gamma-gamma fading channels, respectively.

We Considered the correlation between the received signals across the different branches of SSC receiver. Substituting $F_{\chi_1,\chi_2}\left(\chi, \chi_{S_{Th}}\right)$ and $F_{\chi_i}\left(\chi\right)$ into (24) and following the derivation steps provided in Appendix E, the closed-form expression for the probability of detection $P_d$ is obtained as

$$\begin{aligned} P_d = {} & \frac{\left(a_V b_V\right)^3 \left(a_R+2\right)\left(b_R+2\right)}{4\left[\Gamma\left(a_V\right)\Gamma\left(b_V\right)\right]^3 \left(a_R b_R\right)^2} \\ & \times \frac{\left(1-\rho^2\right)^{b_R}}{\left[\Gamma\left(a_R\right)\right]^2 \Gamma\left(b_R\right)} \sum_{i=0}^{\infty} \frac{1}{\Gamma\left(b_R+i\right) i!} \Xi^{(a_R+b_R+i)} \rho^{2i} \\ & \times \left\{ \frac{\left(a_V b_V\right)\left(a_R+2\right)\left(b_R+2\right)}{\Gamma\left(a_V\right)\Gamma\left(b_V\right)\left(a_R b_R\right)^2} \right\}^{\left(\frac{a_R+b_R+i}{2}-1\right)} \\ & \times G_{1,3}^{2,1}\left[ \frac{\chi_{Th}}{\xi} M \middle| \begin{matrix} 1-\frac{a_R+b_R+i}{4} \\ \frac{b_R+i-a_R}{2}, -\frac{b_R+i-a_R}{2}, -\frac{a_R+b_R+i}{4} \end{matrix} \right] \\ & \times G_{1,3}^{2,1}\left[ \frac{\chi_{S_{Th}}}{\xi} M \middle| \begin{matrix} 1-\frac{a_R+b_R+i}{4} \\ \frac{b_R+i-a_R}{2}, -\frac{b_R+i-a_R}{2}, -\frac{a_R+b_R+i}{4} \end{matrix} \right] \\ & \times \left( \frac{\chi_{Th}\chi_{S_{Th}}}{\xi} \right)^{\left(\frac{a_R+b_R+i}{4}\right)}, \quad \chi_{Th} \le \chi_{S_{Th}}. \end{aligned} \quad (29)$$

## V. SIMULATION RESULTS AND ANALYSIS

We quantify the sensing performance of the proposed system by depicting the probability of detection and probability of false alarm. A UV wavelength equal to 260 nm is considered for the communication link. $C_n^2$ is assumed to be constant and set to $5 \times 10^{-15}$ m$^{-2/3}$. $\phi_t$ and $\phi_r$ are set to $\pi/180$ and $\pi/4$, respectively. $\psi_t$ and $\psi_r$ are both set to $\pi/3$. All the angles are measured in radians. $A_r$ is set to 1.77 cm$^2$. $\alpha_t$ is set to 0.802 km$^{-1}$ and $\alpha_s$ is equal to 0.266 km$^{-1}$ [22]. $\sigma_{n,Th}^2$ is set to 1 and $\chi_{Th}$ is set to 5 dB.

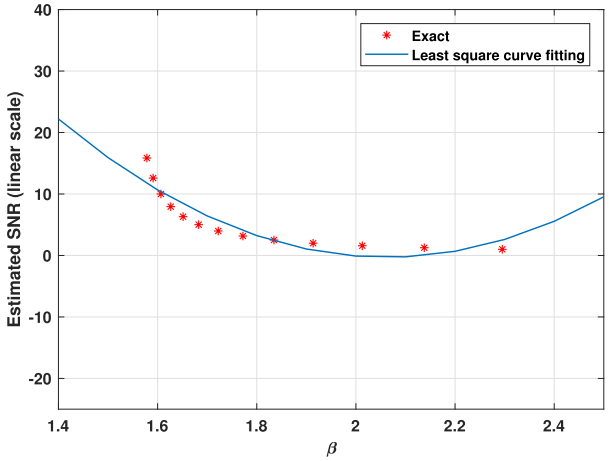


**FIGURE 3.** SNR estimation based on the statistical ratio $\beta$.

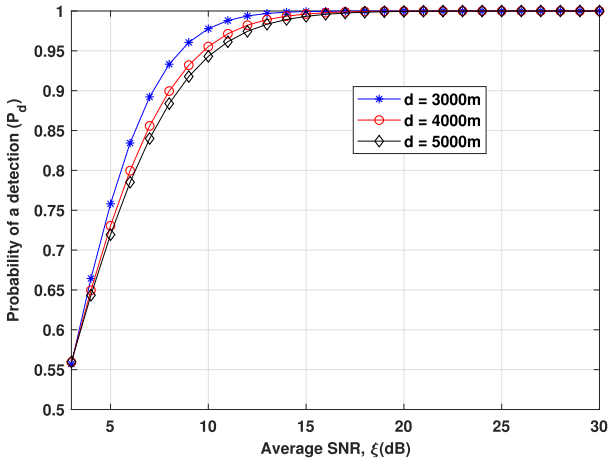


**FIGURE 4.** Probability of detection relative to the average received SNR.

An approximate relation between $\beta$ and $\xi$ can be obtained through a polynomial curve fitting. The estimated SNR value is compared with the exact SNR in Fig. (3). To find the estimated SNR values, we used the least square curve fitting method based on the statistical ratio $\beta$. In the least square estimation, it should be noted that the squared discrepancies between the received UV signals and their expected value are minimized. Another estimation method may include a least absolute deviation method for parameter estimation.

The probability of detection relative to the average SNR for different baseline distances are depicted in Fig. (4). As the baseline distance increases, the correlated UV signals experience more path loss, thereby resulting in poor system performance.

In Fig. (5), the performance of the proposed scheme for different values of the correlation coefficient is presented. The result for no correlation case is also presented. As it is expected, the optical link with diversity branches has the best

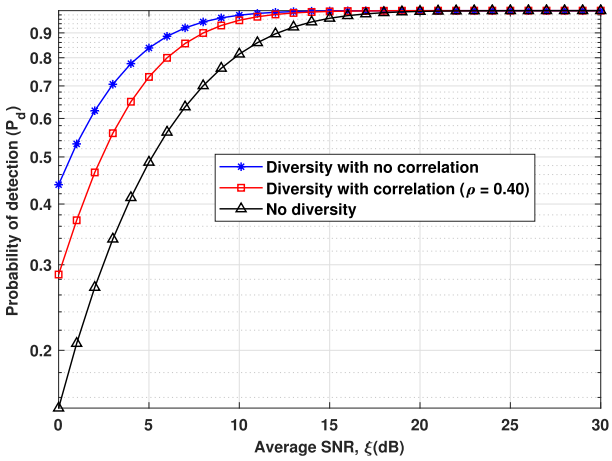


**FIGURE 5.** Probability of detection relative to the average received SNR.

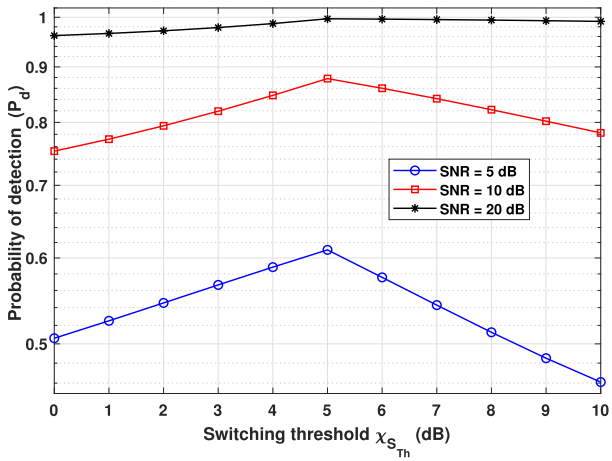


**FIGURE 6.** Probability of detection relative to the switching threshold.

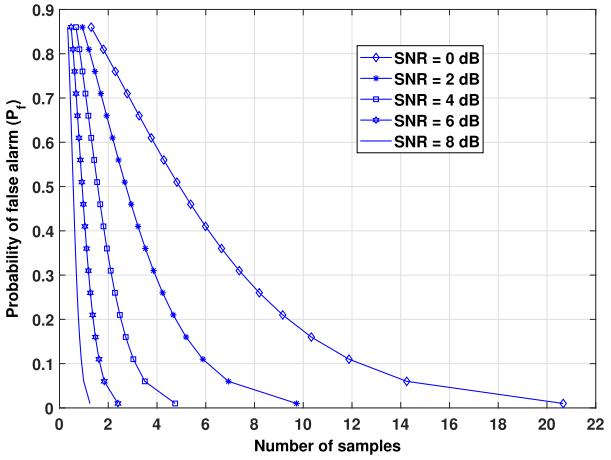


**FIGURE 7.** Probability of false alarm relative to the number of samples.

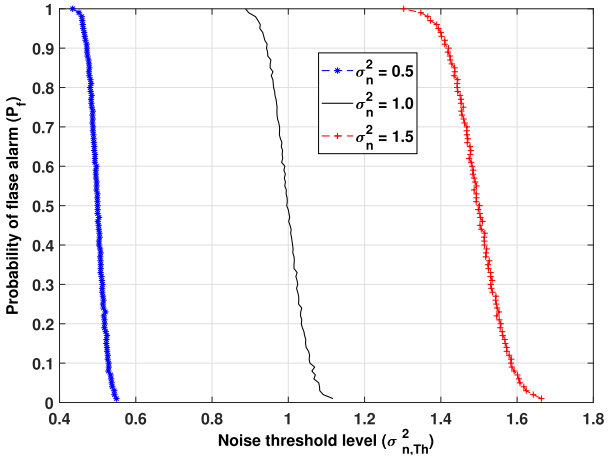


**FIGURE 8.** Probability of false alarm relative to the noise threshold level.

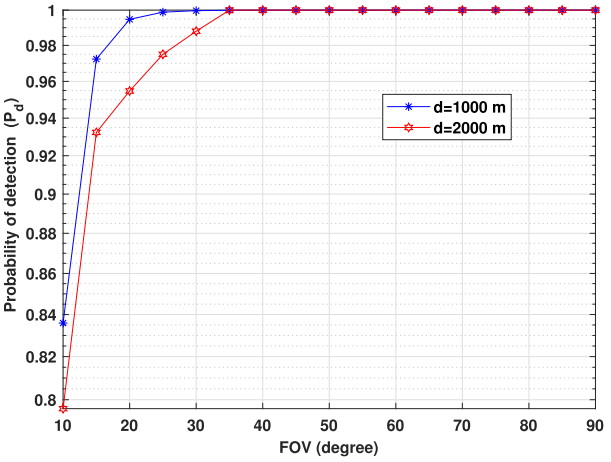


**FIGURE 9.** Probability of detection relative to the receiver FOV.

performance. Also, it can be seen that when the correlation coefficient is changed from zero to 0.40, the penalty in electrical SNR should be paid by approximately 2 dB in the low SNR regime.

The considerable effect of the appropriate selection of the switching threshold on the probability of detection is depicted in Fig. (6). It can be seen that there exists an optimum switching threshold value that maximizes the detection probability. This optimum value is found to be equal to the decision threshold.

Fig. (7) illustrates the probability of false alarm as a function of the number of samples. To observe the impact of the number of samples, we varied the number of samples over the fixed SNR values. It is found that for the given SNR, the probability of false alarm decreases with increasing number of samples.

Fig. (8) plots the probability of false alarm as a function of the noise threshold level $\sigma^2_{n,Th}$. It presents a range of noise threshold level that should be chosen in order to meet a specific probability of false alarm. An optimal detection threshold is required for efficient spectrum sensing. The selection of the threshold detection in the proposed scheme depends on the knowledge of the estimated noise power, and therefore an inaccurate estimation of the noise power level can lead to a high probability of false alarm.

The performance of the proposed system against the receiver FOV is depicted in Fig. (9). FOV is one of the important parameters to investigate the impact of user geometry. The performance of the proposed system is found to be sensitive at low FOV values. This can be attributed to the

fact that as the FOV increases, more energy is collected at the receiver, thereby resulting in a high received SNR.

The proposed scheme does not need any information of the optical signal to be sensed and shows a high gain in the unknown dispersive channel. As compared with the conventional spectrum sensing schemes including matched filter detection and covariance-based detection, the proposed scheme can be applied to both narrowband and wideband sensings. In addition, it has low complexity as no continuous monitoring of all the received branches is required in the SSC combiner.

## VI. CONCLUSION

In this paper, a new blind spectrum sensing scheme of an ultraviolet link under strong atmospheric turbulence fading channel is presented. This new scheme makes use of the statistical ratio of the received signal that is used to estimate the SNR and noise power. The estimated SNR and noise power are then used to evaluate the probability of detection and the probability of false alarm, respectively. The irradiance fluctuations are assumed to follow a gamma-gamma distribution. The novel analytical expressions for the probability of detection and the probability of false alarm have been obtained. We have also quantified the improvement in the ultraviolet spectrum sensing capability when the receiver diversity scheme is employed. Numerical results are presented to validate that the proposed scheme can guarantee a reliable ultraviolet spectrum sensing performance while enhancing the spectrum utilization efficiency. Future work may include to find an optimal solution for the optimum switching threshold to maximize the probability of detection.

## APPENDICES A
## MARGINAL PDF OF THE RECEIVED IRRADIANCE FLUCTUATIONS

In this section, we derive a closed-form analytical expression for the PDF of the marginal PDF of received irradiance fluctuations in a NLOS UV link geometry. Substituting (6) and (7) into (8), and using the identity [18, eq. (14)],

$$K_v(x) = \frac{1}{2} G_{0,2}^{2,0}\left\{ \frac{x^2}{4} \middle| \begin{matrix} - \\ \frac{v}{2}, -\frac{v}{2} \end{matrix} \right\}, \tag{30}$$

(8) can then be written as

$$\begin{aligned} f_{I_R}(I_R) &= \frac{2\left(a_V b_V\right)^{\left(\frac{a_V+b_V}{2}\right)} \left(a_R b_R\right)^{\left(\frac{a_R+b_R}{2}\right)}}{\Gamma(a_V)\,\Gamma(b_V)\,\Gamma(a_R)\,\Gamma(b_R)} \\ &\quad \times I_R^{\left(\frac{a_R+b_R-2}{2}\right)} G_{0,2}^{2,0}\left[ a_R b_R I_R \middle| \begin{matrix} \frac{a_R-b_R}{2}, - \\ - \end{matrix} \frac{a_R-b_R}{2} \right] \\ &\quad \times \int_0^\infty I_V^{\left(\frac{a_V+b_V-2}{2}\right)} \\ &\quad \times G_{0,2}^{2,0}\left[ a_V b_V I_V \middle| \begin{matrix} \frac{a_V-b_V}{2}, - \\ - \end{matrix} \frac{a_V-b_V}{2} \right] dI_V, \end{aligned} \tag{31}$$

Integrating (31) using the identity [16, eq. 7.811.4]

$$\begin{aligned} &\int_0^\infty x^{\rho-1} G_{p,q}^{m,n}\left\{ \alpha x \middle| \begin{matrix} a_1, \ldots, a_p \\ b_1, \ldots, b_q \end{matrix} \right\} dx \\ &= \frac{\prod_{j=1}^{m} \Gamma\left(b_j+\rho\right) \prod_{j=1}^{n} \Gamma\left(1-a_j-\rho\right)}{\prod_{j=m+1}^{q} \Gamma\left(1-b_j-\rho\right) \prod_{j=n+1}^{p} \Gamma\left(a_j+\rho\right)} \alpha^{-\rho}, \end{aligned} \tag{32}$$

the closed-form expression is obtained as

$$\begin{aligned} f_{I_R}(I_R) &= \frac{2\left(a_V b_V\right)^{\left(\frac{a_V+b_V}{2}\right)} \left(a_R b_R\right)^{\left(\frac{a_R+b_R}{2}\right)}}{\Gamma(a_V)\,\Gamma(b_V)\,\Gamma(a_R)\,\Gamma(b_R)} \\ &\quad \times I_R^{\left(\frac{a_R+b_R-2}{2}\right)} K_{a_R-b_R}\left(2\sqrt{a_R b_R I_R}\right) \\ &\quad \times \left(a_V\right)^{1-\left(\frac{a_V+b_V}{2}\right)} \left(b_V\right)^{1-\left(\frac{a_V+b_V}{2}\right)}. \end{aligned} \tag{33}$$

After applying simple mathematical manipulations, the simplified closed-form expression for the PDF of $I_R$ is obtained as given by (9).

## APPENDICES B
## DERIVATION OF $E[y^2]$

$E[I_R^2]$ in (13) denotes the second-moment of $I_R$. Following the definition of second-moment

$$E\left[I_R^2\right] = \int_0^\infty I_R^2 f_{I_R}(I_R)\, dI_R, \quad I_R > 0. \tag{34}$$

Substituting (9) into (34) and using the identity [18, eq. (14)], we obtain

$$\begin{aligned} E\left[I_R^2\right] &= \frac{\left(a_V b_V\right)\left(a_R b_R\right)^{\left(\frac{a_R+b_R}{2}\right)}}{\Gamma(a_V)\,\Gamma(b_V)\,\Gamma(a_R)\,\Gamma(b_R)} \times \int_0^\infty I_R^{\left(\frac{a_R+b_R+2}{2}\right)} \\ &\quad \times G_{0,2}^{2,0}\left[ a_R b_R I_R \middle| \begin{matrix} \frac{a_R-b_R}{2}, - \\ - \end{matrix} -\frac{a_R-b_R}{2} \right] dI_R. \end{aligned} \tag{35}$$

Using identity [16, eq. 7.811.4] and integrating (35), the closed-form expression for $E\left[I_R^2\right]$ is obtained as

$$E\left[I_R^2\right] = \frac{\left(a_V b_V\right)}{\Gamma(a_V)\,\Gamma(b_V)} \left(\frac{a_R+2}{a_R^2}\right)\left(\frac{b_R+2}{b_R^2}\right). \tag{36}$$

Substituting (36) into (13) and using the facts $E[w^2] = \sigma_n^2$ and $E[w] = 0$, the closed-form expression for $E[y^2]$ is obtained as shown in (14).

## APPENDICES C
## DERIVATION OF $E[y]$

Since $P_r$ is independent of $I$ and $w$ and also can take two equally likely outcomes 0 or $P_r$, the expected value of $y$ over $P_r$ is then given as

$$\begin{aligned} E\left[y \,|w_i, I_{Ri}\right] &= \frac{1}{2} E\left[SP_r I_{Ri} + w_i\right] + \frac{1}{2} E\left[w_i\right] \\ &= \frac{1}{2} E\left[SP_r I_{Ri} + w_i\right]. \end{aligned} \tag{37}$$

Now, by averaging Gaussian noise $w_i$ conditioned on $I_i$, we obtain

$$E\left[y_i \left| I_{Ri}=I_R\right.\right]=\frac{1}{\sqrt{2\pi\sigma_n^2}}\int_{-\infty}^{\infty}\left(SP_rI_R+w\right)e^{-\frac{w^2}{2\sigma_n^2}}dw. \quad (38)$$

Using identities [16, eqs. 3.323.2 and 3.426.6], (38) can be reduced to

$$E\left[y_i \left| I_{Ri}=I_R\right.\right]=\frac{SP_rI_R}{2}. \quad (39)$$

Taking the expectation of (39) over $I_R$, we obtain

$$E\left[y_i\right]=\frac{SP_r}{2}\int_0^{\infty}I_Rf_{I_R}\left(I_R\right)dI_R, I_R>0. \quad (40)$$

Substituting (9) into (40) and using [18, eq. (14)], we obtain

$$E\left[y_i\right]=\frac{SP_r\left(a_Vb_V\right)\left(a_Rb_R\right)^{\left(\frac{a_R+b_R}{2}\right)}}{2\Gamma\left(a_V\right)\Gamma\left(b_V\right)\Gamma\left(a_R\right)\Gamma\left(b_R\right)}\times\int_0^{\infty}I_R^{\left(\frac{a_R+b_R}{2}\right)}\times G_{0,2}^{2,0}\left[a_Rb_RI_R\left|\begin{matrix}\frac{a_R-b_R}{2},-\frac{a_R-b_R}{2}\end{matrix}\right.\right]dI_R. \quad (41)$$

Using identity [16, eq. 7.811.4], the closed-form expression for $E[y]$ is obtained as provided in (15).

## APPENDICES D
## DERIVATION OF THE CDF OF THE INSTANTANEOUS SNR

Using (10) and (11), we obtain

$$I_R=\sqrt{\left(\frac{\chi_i}{\xi}\right)\frac{\left(a_Vb_V\right)}{\Gamma\left(a_V\right)\Gamma\left(b_V\right)}\left(\frac{a_R+2}{a_R^2}\right)\left(\frac{b_R+2}{b_R^2}\right)}. \quad (42)$$

On taking the Jacobean transformation of (46) defined as $|J|=\left|\frac{\partial I_R}{\partial\chi_i}\right|$, the marginal PDF of the instantaneous SNR $\chi_i$ is then given by

$$f_{\chi_i}\left(\chi_i\right)=|J|f_{I_R}\left(I_R\right)\left|_{I_R=\sqrt{\left(\frac{\chi_i}{\xi}\right)\frac{\left(a_Vb_V\right)}{\Gamma\left(a_V\right)\Gamma\left(b_V\right)}\left(\frac{a_R+2}{a_R^2}\right)\left(\frac{b_R+2}{b_R^2}\right)}}\right.. \quad (43)$$

On substituting the values, the closed-form expression for the marginal PDF of the instantaneous SNR is obtained as

$$f_{\chi_i}\left(\chi\right)=\left(\frac{a_Vb_V}{\Gamma\left(a_V\right)\Gamma\left(b_V\right)}\right)^{\left(\frac{a_R+b_R+4}{4}\right)}\frac{\left[\left(a_R+2\right)\left(b_R+2\right)\right]^{\left(\frac{a_R+b_R}{4}\right)}}{\Gamma\left(a_V\right)\Gamma\left(b_V\right)}\times G_{0,2}^{2,0}\left[\sqrt{\frac{a_Vb_V\left(a_R+2\right)\left(b_R+2\right)\chi_i}{\Gamma\left(a_V\right)\Gamma\left(b_V\right)\xi}}\left|\begin{matrix}\frac{a_R-b_R}{2},-\frac{a_R-b_R}{2}\end{matrix}\right.\right]\times\frac{\chi_i^{\left(\frac{a_R+b_R+4}{4}\right)}}{\xi^{\left(\frac{a_R+b_R}{4}\right)}}. \quad (44)$$

The CDF of $\chi_i$ is defined as

$$F_{\chi_i}\left(\chi\right)=\int_0^{\chi}f_{\chi_i}\left(\chi\right)d\chi. \quad (45)$$

Integrating (45) using identity [18, eq. 26], the closed-form expression for $F_{\chi_i}\left(\chi\right)$ is derived as provided in (25).

## APPENDICES E
## DERIVATION OF THE PROBABILITY OF DETECTION

Following the steps provided in [21] and [23], the joint PDF of irradiance at the SSC receiver is derived as

$$f_{I_{R1},I_{R2}}\left(I_{R1},I_{R2}\right)=\frac{4\left(a_Vb_V\right)^2}{\left[\Gamma\left(a_V\right)\Gamma\left(b_V\right)\right]^2}\times\frac{\left(1-\rho^2\right)^{b_R}}{\left[\Gamma\left(a_R\right)\right]^2\Gamma\left(b_R\right)}\sum_{i=0}^{\infty}\frac{1}{\Gamma\left(b_R+i\right)i!}\times\Xi^{\left(a_R+b_R+i\right)}\rho^{2i}\times I_{R1}^{\left(\frac{a_R+b_R+i}{2}-1\right)}K_{b_R+i-a_R}\left(2\sqrt{\Xi I_{R1}}\right)\times I_{R2}^{\left(\frac{a_R+b_R+i}{2}-1\right)}K_{b_R+i-a_R}\left(2\sqrt{\Xi I_{R2}}\right), \quad (46)$$

where $\Xi=\frac{ab}{(1-\rho^2)E[I_R]}$.

Using (10) and (11), and applying the Jacobean transformation the joint PDF of the instantaneous SNR is obtained as

$$f_{\chi_1,\chi_2}\left(\chi_1,\chi_2\right)=|J|f_{I_{R1},I_{R2}}\left(I_{R1},I_{R2}\right), \quad (47)$$

where $|J|$ is the Jacobean matrix defined as

$$|J|=\left|\begin{matrix}\frac{\partial I_{R1}}{\partial\chi_1} & \frac{\partial I_{R1}}{\partial\chi_2}\\ \frac{\partial I_{R2}}{\partial\chi_1} & \frac{\partial I_{R2}}{\partial\chi_2}\end{matrix}\right|, \text{ where}$$

$$\frac{\partial I_{Ri}}{\partial\chi_j}=\begin{cases}\frac{1}{2\sqrt{\chi_i\xi}}\sqrt{\frac{\left(a_Vb_V\right)}{\Gamma\left(a_V\right)\Gamma\left(b_V\right)}\left(\frac{a_R+2}{a_R^2}\right)\left(\frac{b_R+2}{b_R^2}\right)}, & i=j\\ 0, & i\neq j.\end{cases} \quad (48)$$

Substituting (46) and (48) into (47) and after some mathematical manipulations, the closed-form expression for the joint PDF of the instantaneous SNR is obtained as

$$f_{\chi_1,\chi_2}\left(\chi_1,\chi_2\right)=\frac{\left(a_Vb_V\right)^3\left(a_R+2\right)\left(b_R+2\right)}{\left[\Gamma\left(a_V\right)\Gamma\left(b_V\right)\right]^3\left(a_Rb_R\right)^2}\times\frac{\left(1-\rho^2\right)^{b_R}}{\left[\Gamma\left(a_R\right)\right]^2\Gamma\left(b_R\right)}\sum_{i=0}^{\infty}\frac{1}{\Gamma\left(b_R+i\right)i!}\Xi^{\left(a_R+b_R+i\right)}\rho^{2i}\times\left\{\frac{\left(a_Vb_V\right)\left(a_R+2\right)\left(b_R+2\right)}{\Gamma\left(a_V\right)\Gamma\left(b_V\right)\left(a_Rb_R\right)^2}\right\}^{\left(\frac{a_R+b_R+i}{2}-1\right)}$$

$$\times K_{b_R+i-a_R}\left(2\sqrt{\Xi\sqrt{\frac{(a_Vb_V)(a_R+2)(b_R+2)}{\Gamma(a_V)\Gamma(b_V)(a_Rb_R)^2}\frac{\chi_1}{\xi}}}\right)$$
$$\times K_{b_R+i-a_R}\left(2\sqrt{\Xi\sqrt{\frac{(a_Vb_V)(a_R+2)(b_R+2)}{\Gamma(a_V)\Gamma(b_V)(a_Rb_R)^2}\frac{\chi_2}{\xi}}}\right)$$
$$\times(\chi_1\chi_2)^{\left(\frac{a_R+b_R+i-4}{4}\right)}\left(\frac{1}{\xi}\right)^{\left(\frac{a_R+b_R+i}{4}\right)}. \quad (49)$$

Using identity [18, eq. (14)], (49) can then be written as

$$f_{\chi_1,\chi_2}(\chi_1,\chi_2) = \frac{(a_Vb_V)^3(a_R+2)(b_R+2)}{4[\Gamma(a_V)\Gamma(b_V)]^3(a_Rb_R)^2}$$
$$\times\frac{\left(1-\rho^2\right)^{b_R}}{[\Gamma(a_R)]^2\Gamma(b_R)}\sum_{i=0}^{\infty}\frac{1}{\Gamma(b_R+i)\,i!}\Xi^{(a_R+b_R+i)}\rho^{2i}$$
$$\times\left\{\frac{(a_Vb_V)(a_R+2)(b_R+2)}{\Gamma(a_V)\Gamma(b_V)(a_Rb_R)^2}\right\}^{\left(\frac{a_R+b_R+i}{2}-1\right)}$$
$$\times G_{0,2}^{2,0}\left[\Xi\sqrt{\frac{(a_Vb_V)(a_R+2)(b_R+2)}{\Gamma(a_V)\Gamma(b_V)(a_Rb_R)^2}\frac{\chi_1}{\xi}}\right.$$
$$\times\left.\left|\frac{b_R+i-a_R}{2},\frac{-}{\frac{a_R-i-b_R}{2}}\right.\right]$$
$$\times G_{0,2}^{2,0}\left[\Xi\sqrt{\frac{(a_Vb_V)(a_R+2)(b_R+2)}{\Gamma(a_V)\Gamma(b_V)(a_Rb_R)^2}\frac{\chi_2}{\xi}}\right.$$
$$\times\left.\left|\frac{b_R+i-a_R}{2},\frac{-}{\frac{a_R-i-b_R}{2}}\right.\right]$$
$$\times(\chi_1\chi_2)^{\left(\frac{a_R+b_R+i-4}{4}\right)}\left(\frac{1}{\xi}\right)^{\left(\frac{a_R+b_R+i}{4}\right)}. \quad (50)$$

Substituting (50) into (26) and solving the double integration using identity [18, eq. 26], $F_{\chi_1,\chi_2}(\chi,\chi_{s,Th})$ can then readily be derived as

$$F_{\chi_1,\chi_2}(\chi,\chi_{S_{Th}}) = \frac{(a_Vb_V)^3(a_R+2)(b_R+2)}{4[\Gamma(a_V)\Gamma(b_V)]^3(a_Rb_R)^2}$$
$$\times\frac{\left(1-\rho^2\right)^{b_R}}{[\Gamma(a_R)]^2\Gamma(b_R)}\sum_{i=0}^{\infty}\frac{1}{\Gamma(b_R+i)\,i!}\Xi^{(a_R+b_R+i)}\rho^{2i}$$
$$\times\left\{\frac{(a_Vb_V)(a_R+2)(b_R+2)}{\Gamma(a_V)\Gamma(b_V)(a_Rb_R)^2}\right\}^{\left(\frac{a_R+b_R+i}{2}-1\right)}$$
$$\times G_{1,3}^{2,1}\left[\frac{\chi}{\xi}M\left|\begin{matrix}1-\frac{a_R+b_R+i}{4}\\ \frac{b_R+i-a_R}{2},-\frac{b_R+i-a_R}{2},-\frac{a_R+b_R+i}{4}\end{matrix}\right.\right]$$
$$\times G_{1,3}^{2,1}\left[\frac{\chi_{S_{Th}}}{\xi}M\left|\begin{matrix}1-\frac{a_R+b_R+i}{4}\\ \frac{b_R+i-a_R}{2},-\frac{b_R+i-a_R}{2},-\frac{a_R+b_R+i}{4}\end{matrix}\right.\right]$$
$$\times\left(\frac{\chi\chi_{S_{Th}}}{\xi}\right)^{\left(\frac{a_R+b_R+i}{4}\right)}, \quad (51)$$

where $M$ is defined as

$$M=\Xi\sqrt{\frac{(a_Vb_V)(a_R+2)(b_R+2)}{\Gamma(a_V)\Gamma(b_V)(a_Rb_R)^2}}. \quad (52)$$

Substituting (51) into (24) and then using (23), the closed-form expression for the probability of detection is then obtained as shown in (29).

## REFERENCES

[1] M. Uysal, C. Capsoni, Z. Ghassemlooy, A. Boucouvalas, and E. Udvary, *Optical Wireless Communications: An Emerging Technology*. Cham, Switzerland: Springer, 2016.
[2] S. Arya and Y. H. Chung, "Non-line-of-sight ultraviolet communication with receiver diversity in atmospheric turbulence," *IEEE Photon. Technol. Lett.*, vol. 30, no. 10, pp. 895–898, May 15, 2018.
[3] G. A. Shaw, A. M. Siegel, and J. Model, "Ultraviolet comm links for distributed sensor systems," *IEEE LEOS Newslett.*, vol. 19, no. 5, pp. 26–29, Oct. 2005.
[4] Z. Xu and B. M. Sadler, "Ultraviolet communications: Potential and state-of-the-art," *IEEE Commun. Mag.*, vol. 46, no. 5, pp. 67–73, May 2008.
[5] C. Gong and Z. Xu, "Temporal spectrum sensing for optical wireless scattering communications," *IEEE Commun. Mag.*, vol. 46, no. 18, pp. 3890–3900, Sep. 2015.
[6] X. Liu, C. Gong, and Z. Xu, "Sequential detection for optical wireless scattering communication," *J. Opt. Commun. Netw.*, vol. 9, no. 9, pp. D86–D95, 2017.
[7] L. C. Andrews and R. L. Phillips, *Laser Beam Propagation Through Random Media*, vol. 152. Bellingham, WA, USA, SPIE, 2005.
[8] W. O. Popoola and Z. Ghassemlooy, "BPSK subcarrier intensity modulated free-space optical communications in atmospheric turbulence," *IEEE/OSA J. Lightw. Technol.*, vol. 27, no. 8, pp. 967–973, Apr. 15, 2009.
[9] Z. Ghassemlooy, W. Popoola, and S. Rajbhandari, *Optical Wireless Communications: System and Channel Modelling with MATLAB*. Boca Raton, FL, USA: CRC Press, 2013.
[10] P. Wang and Z. Xu, "Characteristics of ultraviolet scattering and turbulent channels," *Opt. Lett.*, vol. 38, no. 15, pp. 2773–2775, 2013.
[11] C. Gong, B. Huang, and Z. Xu , "Correlation and outage probability of NLOS SIMO optical wireless scattering communication channels under turbulence," *IEEE/OSA J. Opt. Commun. Netw.*, vol. 8, no. 12, pp. 928–937, Dec. 2016.
[12] H. Ding, "Modeling and characterization of ultraviolet scattering communication channels," Ph.D. dissertation, Dept. Elect. Eng., Univ. California, Riverside, Riverside, CA, USA, 2011.
[13] H. Ding, G. Chen, A. K. Majumdar, B. M. Sadler, and Z. Xu, "Turbulence modeling for non-line-of-sight ultraviolet scattering channels," *Proc. SPIE*, vol. 8038, no. 5, 2011, Art. no. 80380J.
[14] M. H. Ardakani, A. R. Heidarpour, and M. Uysal, "Performance analysis of relay-assisted NLOS ultraviolet communications over turbulence channels," *J. Opt. Commun. Netw.*, vol. 9, no. 1, pp. 109–118, 2017.
[15] T. A. Summers and S. G. Wilson, "SNR mismatch and online estimation in turbo decoding," *IEEE Trans. Commun.*, vol. 46, no. 4, pp. 421–423, Apr. 1998.
[16] I. S. Gradshteyn and I. M. Ryzhik, *Table of Integrals, Series, and Products*. New York, NY, USA: Academic, 2014.
[17] J. G. Proakis and M. Salehi, *Digital Communications*. New York, NY, USA: McGraw-Hill, 2008.
[18] V. S. Adamchik and O. I. Marichev, "The algorithm for calculating integrals of hypergeometric type functions and its realization in REDUCE system," in *Proc. Int. Symp. Symbolic Algebr. Comput.*, 1990, pp. 212–224.
[19] G. Yang, M.-A. Khalighi, Z. Ghassemlooy, and S. Bourennane, "Performance evaluation of receive-diversity free-space optical communications over correlated Gamma–Gamma fading channels," *Appl. Opt.*, vol. 52, no. 24, pp. 5903–5911, 2013.
[20] G. Yang, M.-A. Khalighi, and S. Bourennane, "Performance of receive diversity FSO systems under realistic beam propagation conditions," in *Proc. 8th Int. Symp. Commun. Syst., Netw. Digit. Signal Process. (CSNDSP)*, 2012, pp. 1–5.
[21] M. Uysal, S. M. Navidpour, and J. Li, "Error rate performance of coded free-space optical links over strong turbulence channels," *IEEE Commun. Lett.*, vol. 8, no. 10, pp. 635–637, Oct. 2004.
[22] H. Ding, G. Chen, Z. Xu, and B. M. Sadler, "Channel modelling and performance of non-line-of-sight ultraviolet scattering communications," *IET Commun.*, vol. 6, no. 5, pp. 514–524, 2012.

[23] K. P. Peppas, G. C. Alexandropoulos, C. K. Datsikas, and F. I. Lazarakis, "Multivariate Gamma–Gamma distribution with exponential correlation and its applications in radio frequency and optical wireless communications," *IET Microw., Antennas Propag.*, vol. 5, no. 3, pp. 364–371, 2011.
[24] H. Moradi, H. H. Refai, and P. G. LoPresti, "Switch-and-stay and switch-and-examine dual diversity for high-speed free-space optics links," *IET Optoelectron.*, vol. 6, no. 1, pp. 34–42, 2013.
[25] L. C. Andrews, R. L. Phillips, and C. Y. Hopen, *Laser Beam Scintillation With Applications*, vol. 99. Bellingham, WA, USA: SPIE, 2001.

**SUDHANSHU ARYA** (S'19) received the M.Tech. degree in communications and networks from the National Institute of Technology, Rourkela, India, in 2017. He is currently pursuing the Ph.D. degree in optical communication with Pukyong National University, Busan, South Korea.

**YEON HO CHUNG** (M'93–SM'17) received the M.Sc. from Imperial College London, U.K., in 1992, and the Ph.D. degree from the University of Liverpool, U.K., in 1996. He was a Visiting Professor with Pennsylvania State University, University Park, PA, USA, and also at Chiba University, Japan. He was a Foreign Expert for the GIAN program of the Government of India, in 2017. His research interests include visible light communications, optical wireless communications, optical healthcare systems, and advanced mobile transmission schemes. He is currently a Professor with the Department of Information and Communications Engineering, Pukyong National University, Busan, South Korea. He is a member of the Editorial Board of the *International Journal of Wireless Personal Communications* (Springer) and also the *Internet Technology Letters* (Wiley). He received the Top 2014 Paper Award from the *Transactions on Emerging Telecommunications Technologies* (ETT) (Wiley). He is an Associate Editor of the IEEE ACCESS.